Journal of Magnetism and Magnetic Materials 321 (2009) 861–864

Contents lists available at ScienceDirect

Journal of Magnetism and Magnetic Materials

journal homepage: www.elsevier.com/locate/jmmm

Structure and magnetism of near-stoichiometric FePd nanoparticles

Markus E. Gruner *, Antje Dannenberg

Physics Department and Center for Nanointegration CENIDE, University of Duisburg-Essen, 47048 Duisburg, Germany

ARTICLE INFO

Available online 30 November 2008

PACS:
61.46.Df
75.50.Ss
73.20.At
36.40.Mr

Keywords:
Density functional theory
Binary transition metal nanoparticle
Multiple twinning
Iron–palladium alloy

ABSTRACT

We investigate from first principles the energetic order of single crystalline $L1_0$-ordered and multiply twinned morphologies of FePd nanoparticles close to the stoichiometric composition considering up to 561 atoms. The results are related to previous analogous calculations of FePt and CoPt nanoparticles. We find that compared to the isoelectronic FePt alloy, multiply twinned structures are slightly favored in energy, while the latent tendencies to form a layered antiferromagnetic structure in the $L1_0$ phase are less pronounced.

1. Introduction

During the past years, large efforts have been spent in the fabrication and characterization of binary platinum-based transition metal nanoparticles. One central reason for their popularity is the extremely large magnetocrystalline anisotropy of $L1_0$-ordered bulk FePt and CoPt, which is exceeding the values obtained for contemporary magnetic storage media by more than one order of magnitude, entitling them as potential building blocks for future ultra-high density recording applications [1–3]. However, for the common experimental fabrication procedures, it turned out that the desired hard-magnetic properties are very difficult to achieve for small particle sizes close to the theoretical superparamagnetic limit [4–9]. This has been related to the inability to induce nearly perfect $L1_0$ order by annealing and also to the occurrence of multiply twinned morphologies. These turned out to be strong competitors as they are energetically favored for particle sizes smaller than 3 nm, which has been pointed out recently by large-scale first principles calculations [10].

FePd nanostructures may also be of interest for recording purposes, but they did not attract comparable attention as it exhibits a factor of 4–5 smaller anisotropy in the $L1_0$ phase—which is, however, still large compared to other materials [11–14]. Another potential field of application for Fe–Pd alloys is in sensors and actuators based on the magnetic shape memory effect which is observed in the disordered fct-phase around $Fe_{70}Pd_{30}$ [15,16]. This phase, however, is metastable and only realized by thermal treatment. In equilibrium, $Fe_{70}Pd_{30}$ decomposes into stoichiometric $L1_0$ FePd and body-centered cubic Fe. From the fundamental point of view, FePd alloys are interesting as they are isoelectronic with their Pt-based counterparts and, therefore, allow investigating the influence of the size of one atomic species on the properties of the material.

Spin polarization, the itinerant character of the electrons as well as the importance of structural relaxations make a computationally expensive full *ab initio* treatment necessary to describe the energetic relationship between single-crystalline and non-crystallographic morphologies, which has become recently possible on state-of-the-art supercomputers [10,17,18]. Following the approach previously outlined in Ref. [10], we compare the energies of ideal cuboctahedral, icosahedral and decahedral geometries with a so-called magic number of atoms N, which are defined by the number n of closed geometric shells

$$N = 1/3(10n^3 + 15n^2 + 11n + 3).$$

We will compare morphologies with a fixed composition that corresponds to the $L1_0$ cuboctahedron with alternating Fe and Pd layers along the [0 0 1]-axis. The two (0 0 1) surfaces are covered by one species. The numbers of Fe and Pd atoms in the cluster (N_{Fe} and N_{Pd}) of a given size N are thus not the same and defined by the following relations:

$$N_{Fe} = 1/3(5n^3 + 6n^2 + 4n)$$

and

$$N_{Pd} = 1/3(5n^3 + 9n^2 + 7n + 3).$$

* Corresponding author. Tel.: +49 203 379 3564; fax: +49 203 379 3665.
E-mail address: Markus.Gruner@uni-due.de (M.E. Gruner).

0304-8853/$ - see front matter © 2008 Elsevier B.V. All rights reserved.
doi:10.1016/j.jmmm.2008.11.062

For other perfectly ordered morphologies (radially ordered icosahedra, axially $L1_0$-ordered decahedra) different formation laws hold. To allow comparison, the excess atoms of one species have been distributed randomly over the anti-sites, here.

2. Computational details

The calculations were carried out in the framework of density functional theory (DFT) [19] using the Vienna *ab initio* simulation package (VASP) [20]. The exchange–correlation functional is described within the generalized gradient approximation (GGA), in the formulation of Perdew and Wang [21] (using the spin interpolation Formula of Vosko, Wilk and Nusair [22]); the core electrons are described within the projector augmented wave (PAW) approach [23]. A plane wave cut-off $E_{cut} = 268$ eV was used for the nano-systems, the *k*-space integration restricted to the Γ-point. The $3d^74s^1$ electrons were treated as valence for Fe, the $4d^95s^1$ electrons as valence for Pd. The size of the supercell containing the particle was chosen so that the distance between atoms of the periodic images was exceeding 9 Å. For our bulk calculations, we explicitly included the semicore Fe 3p electrons using the GGA of Perdew Burke and Ernzerhoff [24] and $E_{cut} = 335$ eV. Up to 196 *k*-points in the irreducible Brillouin zone were considered for the smallest cell. The structural relaxations were performed on the Born-Oppenheimer surface using a conjugate gradient scheme. Convergence was assumed when the energy between two consecutive steps dropped below 0.1 meV leading to residual forces of typically 10 meV/Å or smaller.

3. Results

Initial calculations performed in the same fashion as for the FePt case [18] confirm that for $L1_0$ cuboctahedra the termination of the [0 0 1] surfaces with Pd atoms is preferred over a Fe-termination. We, therefore, restrict our investigations to morphologies with predominantly Pd-covered surfaces. The size-dependent evolution of the energetic order of icosahedra, decahedra and $L1_0$-ordered cuboctahedra is shown in Fig. 1. To allow a straightforward comparison, the energies are relative to the $L1_0$ cuboctahedra, which is taken as reference for each size. For the different morphologies, exactly the same compositional distributions are used as in Ref. [10]. The results concerning the ordered multiply twinned morphologies are very similar with a slightly increased tendency to favor the non-crystallographic structures. For $N = 561$, the icosahedron consisting of alternating Fe and Pt-rich shells, which exhibits the lowest energy of the compared morphologies for all sizes, is 43 meV/atom lower in energy than the $L1_0$ isomer as compared to 30 meV/atom in the FePt case. Larger discrepancies are encountered for the disordered icosahedron, which are still now considerably closer to the $L1_0$ reference, reflecting the reduced ordering temperature in the FePd alloy. Another difference to the FePt case is the significance of antiferromagnetic (AF) configurations. Recent DFT calculations for the isoelectronic Fe–Pt system reveal the existence of an AF solution with a slightly reduced *c/a* ratio, which is nearly degenerate in energy with the ferromagnetic (FM) ground state [25–27]. The corresponding configuration consists of alternating ferromagnetic Fe layers with nonmagnetic Pt layers in between which was traced back to the competition between the direct AF interaction between the Fe atoms of different layers and a FM

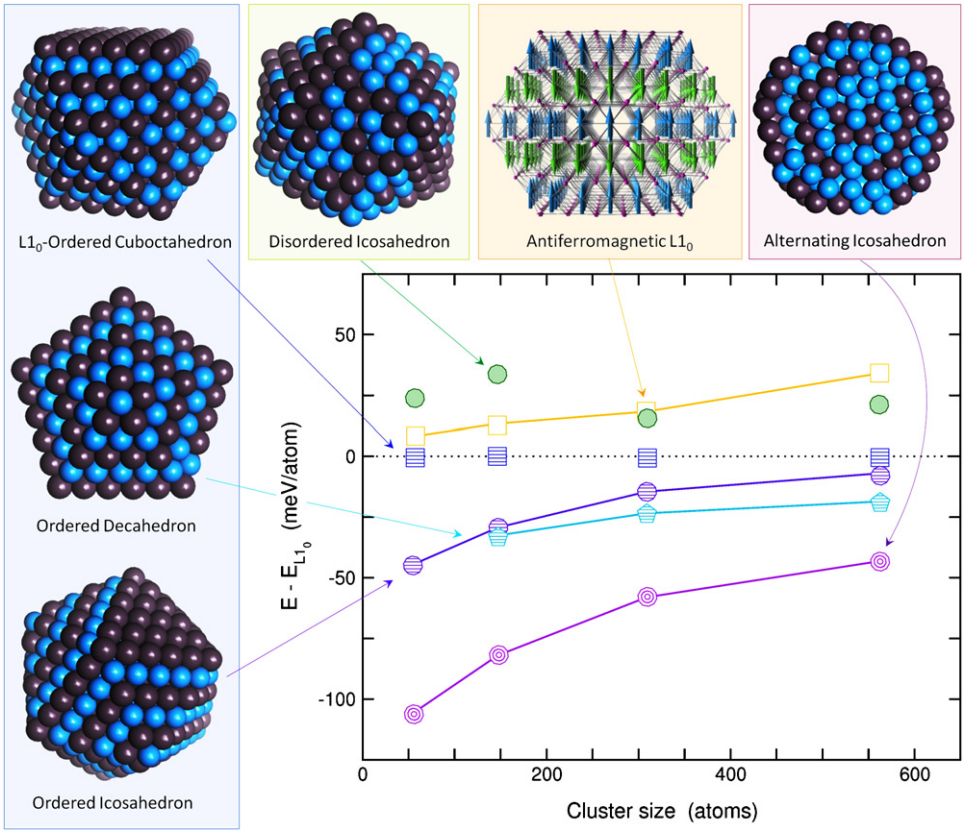

Fig. 1. Energy of various morphologies of FePd nanoparticles as a function of the number of atoms *N* in the particle. The images on the left and on the top refer to the respective morphologies at $N = 561$. Cuboctahedra are represented by squares, decahedra by pentagons and icosahedral morphologies by spheres. All energies are relative to the $L1_0$ cuboctahedron of the respective size. The lines are only guide to the eye.

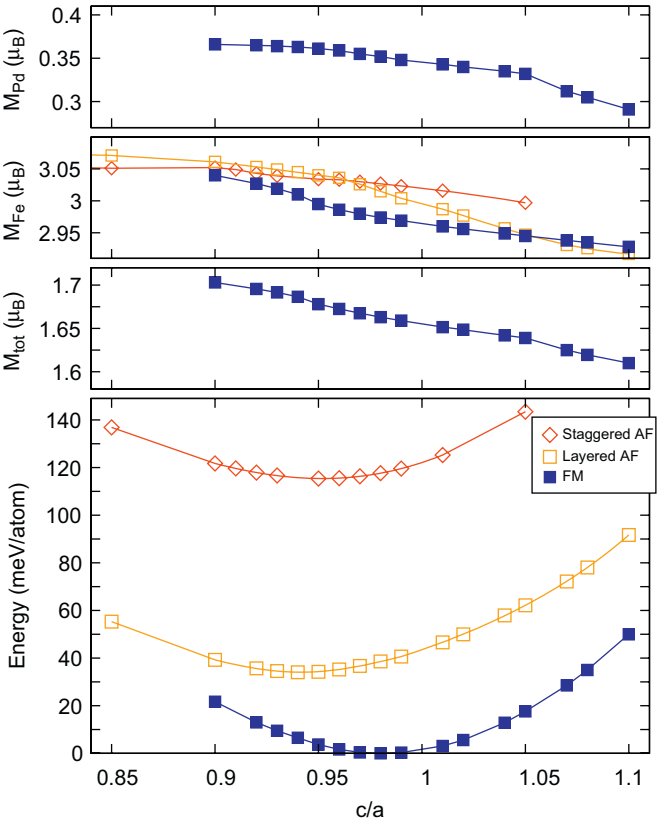

Fig. 2. Energy and magnetic moments as a function of the *c/a* ratio for FM (closed squares) and AF (open symbols, squares for layered, diamonds for staggered AF) configurations of bulk $L1_0$ FePd. All calculations were carried out isochorously at the equilibrium volume of the respective state, which was determined in a separate calculation ($V = 13.94\,Å^3$ for FM, $13.98\,Å^3$ for layered AF and $14.08\,Å^3$ for staggered AF).The total and element resolved absolute magnetic moments are given in Bohr magnetons per atom (of the respective type). The Pd moments in the AF configurations are zero and, thus not shown.

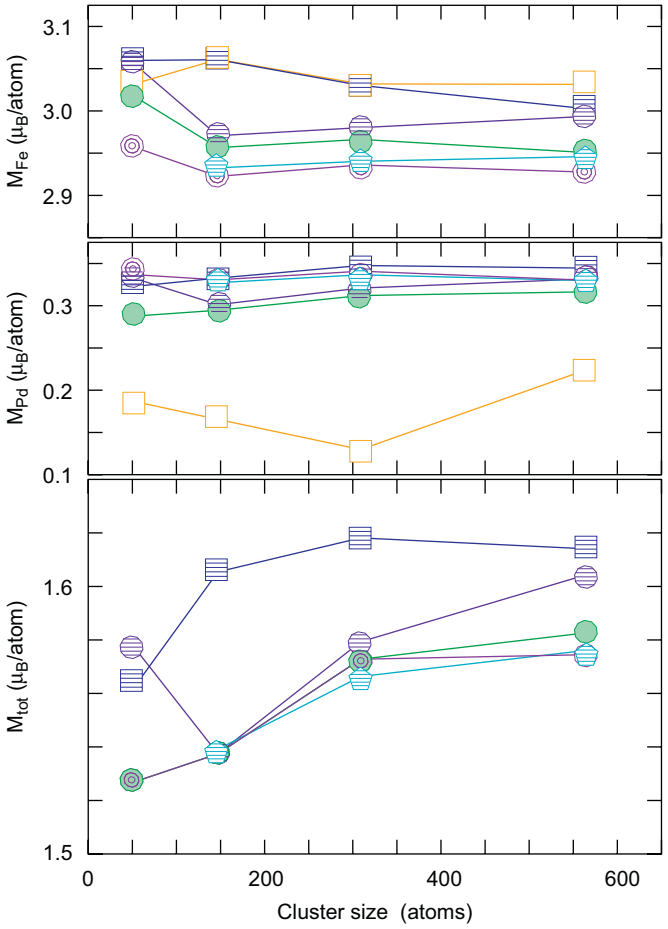

Fig. 3. Size dependence of the (total and element resolved absolute) magnetic moments of FePd nanoclusters for different morphologies. Same symbols as in Fig. 1. The neet spin-polarization of the Pd atoms in the AF configuration is related to surface atoms.

Pt-mediated interaction, while the intra-layer coupling in the Fe-layer is FM [28]. The existence of such a solution can be of importance under extremely strained conditions (which may eventually be encountered due to particle–substrate interactions) [18] or when elements with a tendency to form AF spin structures are co-alloyed. However, magnetocrystalline anisotropy and incomplete $L1_0$ ordering have been shown to support the FM state [25,26]. In $L1_0$ FePd, AF and FM solutions are found to be stable at different *c/a* ratios in a similar fashion, although the layered AF solution is considerably higher in energy (34 meV/atom, cf. Fig. 2) than the FM state, which in contrast to the FePt case. A similar value can be found for the 561 isomers in Fig. 1, while the energy difference is decreasing for decreasing particle sizes. The staggered AF solution of the MnPt type, where the spin orientations of the nearest neighbor Fe atoms are alternating within one layer is another 81 meV/atom higher in energy than the layered AF state.

The absolute values of magnetic moments of the Fe atoms are slightly increased for the AF configurations, while Pd consequently does not show an induced moment. The size-dependent evolution of the magnetic moments as a function of the particle size is shown in Fig. 3. $L1_0$-ordered structures generally posses a higher moment than the non-crystallographic morphologies, the differences, however, are small. The increase of the average magnetic moment with cluster size is related to the variation of the composition, as, especially for Fe, surface atoms have a slightly higher moment.

4. Conclusions

For particle sizes of 561 atoms and below, ordered multiply twinned morphologies as icosahedra and decahedra are favored over single-crystalline $L1_0$-ordered structures. For geometrical reasons, only the latter ones may show hard magnetic behavior suitable for recording purposes. The quantitative relationship between the morphologies bears large similarities to the energy differences obtained for the isoelectronic FePt clusters—except for the disordered structures which are closer to the ordered ones for FePd. Another significant difference is that latent antiferromagnetic tendencies, which were predicted for FePt, appear suppressed. This may be an advantage when designing a suitable material for ultra-high density recording media that should possess a large magnetocrystalline anisotropy, a stable ferromagnetic configuration and a low affinity to form twinned structures. Concerning the size and morphology dependent variation of the magnetic moments, a delicate dependence on composition and structural features, as varying interlayer distances or surface relaxations can be expected. This, however, will be discussed in a future publication.

Acknowledgments

The calculations were carried out on the IBM Blue Gene/L and Blue Gene/P supercomputer systems of the John von Neumann

Institute for Computing at Forschungszentrum Jülich. The substantial support of the staff is gratefully acknowledged. The authors also thank Peter Entel for fruitful discussions. Financial support was granted by the Deutsche Forschungsgemeinschaft via SPP 1239 and SFB 445.

References

[1] M.L. Plumer, J. van Ek, D. Weller (Eds.), The Physics of Ultra-High-Density Magnetic Recording, Springer, Berlin, 2001.
[2] S. Sun, C.B. Murray, D. Weller, L. Folks, A. Moser, Science 287 (2000) 1989.
[3] S. Sun, Adv. Mater. 18 (2006) 393.
[4] B. Stahl, J. Ellrich, R. Theissmann, M. Ghafari, S. Bhattacharya, H. Hahn, N.S. Gajbhiye, D. Kramer, R.N. Viswanath, J. Weissmüller, H. Gleiter, Phys. Rev. B 67 (2003) 014422.
[5] C. Antoniak, J. Lindner, M. Spasova, D. Sudfeld, M. Acet, M. Farle, K. Fauth, U. Wiedwald, H.-G. Boyen, P. Ziemann, F. Wilhelm, A. Rogalev, S. Sun, Phys. Rev. Lett. 97 (2006) 117201.
[6] G.A. Held, H. Zeng, S. Sun, J. Appl. Phys. 95 (2004) 1481.
[7] T. Miyazaki, O. Kitakami, S. Okamoto, Y. Shimada, Z. Akase, Y. Murakami, D. Shindo, Y.K. Takahashi, K. Hono, Phys. Rev. B 72 (2005) 144419.
[8] O. Dmitrieva, B. Rellinghaus, J. Kästner, M.O. Liedke, J. Fassbender, J. Appl. Phys. 97 (2005) 10N112.
[9] R. Wang, O. Dmitrieva, M. Farle, G. Dumpich, H.Q. Ye, H. Poppa, R. Kilaas, C. Kisielowski, Phys. Rev. Lett. 100 (2008) 017205.
[10] M.E. Gruner, G. Rollmann, P. Entel, M. Farle, Phys. Rev. Lett. 100 (2008) 087203.
[11] D. Weller, A. Moser, IEEE Trans. Magn. 35 (1999) 4423.
[12] I. Galanakis, M. Alouani, H. Dreyssé, Phys. Rev. B 62 (2000) 6475.
[13] J.B. Staunton, L. Szunyogh, A. Buruzs, B.L. Gyorrfy, S. Ostanin, L. Udvardi, Phys. Rev. B 74 (2006) 144411.
[14] J. Lyubina, I. Opahle, K.-H. Müller, O. Gutfleisch, M. Richter, M. Wolf, L. Schultz, J. Phys. Condens. Matter. 17 (2005) 4157.
[15] R.D. James, M. Wuttig, Philos. Mag. A 77 (1998) 1273.
[16] J. Cui, T.W. Shield, R.D. James, Acta Materialia 52 (2004) 35.
[17] G. Rollmann, M.E. Gruner, A. Hucht, R. Meyer, P. Entel, M.L. Tiago, J. Chelikowsky, Phys. Rev. Lett. 99 (2007) 083402.
[18] M.E. Gruner, J. Phys. D: Appl. Phys. 41 (2008) 134015.
[19] P. Hohenberg, W. Kohn, Phys. Rev. 136 (1964) B864.
[20] G. Kresse, J. Furthmüller, Phys. Rev. B 54 (1996) 11169.
[21] J.P. Perdew, in: P. Ziesche, H. Eschrig (Eds.), Electronic Structure of Solids '91, Akademie Verlag, Berlin, 1991.
[22] S.H. Vosko, L. Wilk, M. Nusair, Can. J. Phys. 58 (1980) 1200.
[23] G. Kresse, D. Joubert, Phys. Rev. B 59 (1999) 1758.
[24] J. Perdew, K. Burke, M. Ernzerhoff, Phys. Rev. Lett. 77 (1996) 3865.
[25] H. Zeng, R. Sabirianov, O. Mryasov, M.L. Yan, K. Cho, D.J. Sellmyer, Phys. Rev. B 66 (2002) 184425.
[26] G. Brown, B. Kraczek, A. Janotti, T.C. Schulthess, G.M. Stocks, D.D. Johnson, Phys. Rev. B 68 (2003) 052405.
[27] J.M. MacLaren, R.R. Duplessis, R.A. Stern, S. Willoughby, IEEE Trans. Magn. 41 (2005) 4347.
[28] O.N. Mryasov, J. Magn. Magn. Mater. 272 (2004) 800.